

DSC INVESTIGATION OF OXYGEN SUBSYSTEM IN Ba-Y-Cu-O SUPERCONDUCTORS

V. M. Egorov, Yu. M. Baykov, V. A. Bershtein, Yu. P. Stepanov and F. A. Chudnovskii

A. F. IOFFE PHYSICO-TECHNICAL INSTITUTE, RUSSIAN ACADEMY OF SCIENCES, POLYTECHNICHESKAYA ST. 26, ST. PETERSBURG, 194021, RUSSIA

DSC investigations have been performed for a series of compounds $\text{Ba}_2\text{YCu}_3\text{O}_y$ with the oxygen content varying in the range $y = 6.0 \dots 6.9$ by means of various heat treatments at 800–1200 K followed by quenching, or through the chemical extraction of oxygen by placing the sample in dihydrogen at 470–490 K. The sample preserving a constant oxygen content during heating in nitrogen exhibited exothermal effects between 450 and 850 K. It has been shown that the ΔH vs. y function reaches maximum at $y \approx 6.5$. Kinetic measurements have shown that the diffusive mobility of oxygen atoms in the lattice is responsible for these effects, viz. the Arrhenius and cooperative processes of reorganization in the non-equilibrium oxygen subsystem of the bulk.

Keywords: Ba-Y-Cu-O superconductor, DSC

Introduction

After the discovery by Bednorz and Müller [1] of high- T_c oxide superconductors (HTSC), the decisive part played by the oxygen subsystem in the superconducting properties shown by those materials has also been realized. The widely varying oxygen content, due e.g. to the variable valence of copper ($\text{Cu}_x^{+3}\text{Cu}_{1-x}^{+2}$)₃ in the most widespread HTSC systems $\text{Ba}_2\text{YCu}_3\text{O}_y$, allowed researchers to describe the correlation between the transition point into superconducting state T_c and y , etc.

On the other hand, it became clear that the superconducting state of $\text{Ba}_2\text{YCu}_3\text{O}_y$ is not determined by y alone but by the lattice structure, lattice oxygen distribution, oxygen mobility and ordering pattern of the oxygen subsystem.

Some information about lattice state and oxygen distribution under quasi-stationary conditions (when the diffusive mobility of oxygen atoms is frozen) has been obtained through neutron and X-ray diffraction techniques, IRS, NMR, etc.

For instance, the preferable locations for oxygen atoms in the planes of Cu1–O, leading to the formation of chains ...O – Cu1 – O – Cu1... were found [2].

The results in [3] evidence the lack of unambiguous relation between y and HTSC properties. Heat-induced escape of oxygen from $\text{Ba}_2\text{YCu}_3\text{O}_y$ under different conditions, with $y = 6.67$ may lead to $T_c = 60$ K as well as $T_c = 90$ K [4]. In the case of chemical extraction of oxygen with dihydrogen, it is possible to maintain superconducting properties ($T_c = 70$ K) with y falling from 6.9 to 6.3, while annealing at 600 K with the same value of $y = 6.3$ eliminates superconductivity [3].

Differential scanning calorimetry (DSC) can provide the important information on the dynamics of oxygen subsystem behaviour in HTSC.

Earlier the results of calorimetric studies have been published dealing with thermal effects of oxygen absorption and desorption in $\text{Ba}_2\text{YCu}_3\text{O}_y$ [5, 6] which actually are the data on the gas-solid interaction and do not directly deal with the energy changes in this compound. Recently [7–9] we have reported on the possibility of the DSC-based experimental observation of the changes in the energy state of $\text{Ba}_2\text{YCu}_3\text{O}_y$ caused by the reorganization of the non-equilibrium oxygen subsystem in quenched or hydrogen-treated samples, on heating in inert atmosphere. Exothermal effects were detected which cannot be related to the variation of the oxygen content ($y = \text{const}$). This paper is devoted to the presentation of the results of those investigations.

Experimental

$\text{Ba}_2\text{YCu}_3\text{O}_y$ samples were prepared through ceramic process of yttrium oxide, copper oxide and barium carbonate [10], with further annealing in oxygen at 400°C to $y = 6.93$. After that, the samples in the shape of tablets $1.5 \times 2 \times 5 \text{ mm}^3$ or powder with an active surface of $0.2 \text{ m}^2/\text{g}$ were used to obtain samples with variable oxygen content. The latter was modified by means of heating at different temperatures with further quenching [10] or hydrogenation at 470–490 K leading to the chemical extraction of oxygen atoms from the $\text{Ba}_2\text{YCu}_3\text{O}_y$ lattice [3, 4]. The oxygen content was controlled by precision weighing with $\Delta y = 0.01$.

In the former technique, the $\text{Ba}_2\text{YCu}_3\text{O}_y$ samples were exposed to different temperatures (≈ 750 – 1200 K) for five hours and then quenched at the treatment temperature in liquid nitrogen. Figure 1 shows the measured dependence of y upon the temperature of treatment (T_q) in the investigated samples fitted with a linear function. Hence it follows that a decrease in the oxygen content of the samples becomes possible only at $T_q > 630$ K, i.e. at temperatures of oxygen diffusive (atomic) mobility unfreezing (≈ 650 K [12]). In this series y varied from 6.93 to ≈ 6.2 . Hydrogenation led to values of y in the range 6.8–5.9.

The investigation of the conductivity and magnetic susceptibility of the initial samples (oxygen content $y = 6.85$ – 6.93) showed $T_c = 92$ K with transition width within 5 K. With sharp decrease of oxygen concentration, in the hydrogenated

samples superconductivity sustained at lower values of y , e.g. $y \approx 6.3$, while the samples prepared by heating and quenching, lost superconducting properties [3].

The thermal features of the investigated samples were defined through the DSC curves obtained with a Perkin-Elmer DSC-2 instrument in nitrogen while heating in the temperature range 400–850 K at a rate of $v = 5\text{--}40$ deg/min. Sapphire was used to gauge the heat capacity scale, while the temperature scale was gauged by the melting point of lead (600.5) and solid-solid transition in potassium sulphate (858.2 K).

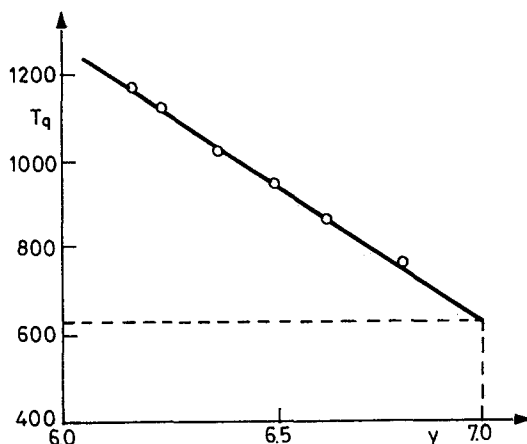


Fig. 1 Dependence of the quenching temperature on the oxygen content in quenched $\text{Ba}_2\text{YCu}_3\text{O}_y$ samples

To increase the sensitivity and accuracy of the measured thermal effect (ΔH), the total heat capacity of an investigated sample was compensated by placing the amorphous quartz sample in the second cell.

Results and discussion

Energetic characteristics of the quenched samples

In Fig. 2 are presented the DSC curves of the quenched samples with different oxygen contents. Apparently, heating in the temperature range 660–860 K is accompanied by a heat release with the highest rate at T_{max} . The exothermal effect is irreversible and missing when scanning is repeated (dashed lines). The enthalpy change ΔH is in proportion with the area between the DSC curves obtained during the first and the second scans. In the quenched samples with extreme values of

$y=6.93$ and 6.19 , there is no exothermal effect: DSC curves measured in two series coincide (not shown in Fig. 2).

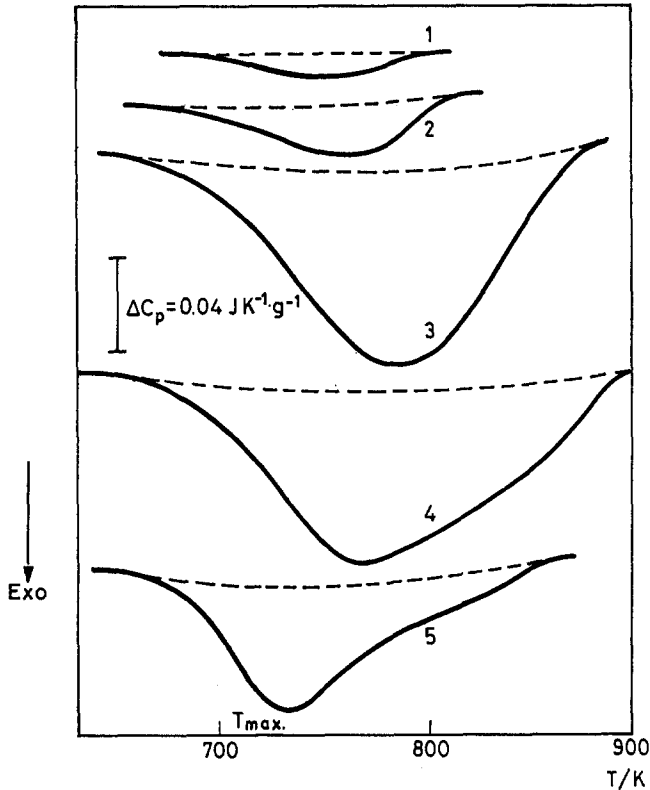


Fig. 2 DSC curves for quenched $\text{Ba}_2\text{YCu}_3\text{O}_y$ samples with different oxygen content: $y=6.81$ (1); 6.73 (2); 6.50 (3); 6.38 (4), and 6.26 (5). Heating rate: 20 deg/min . Dashed lines correspond to scan II.

Check weighing did not show any change in weight, hence the oxygen content of the samples was the same before and after the heat release. In other words, these exothermal effects are not to be related to the interaction processes between the samples and the gaseous phase, but evidence the energy change accompanying some reorganization directly in the solid phase, the release of the latent energy saved as the result of quenching.

Special additional experiments have also evidenced that oxygen absorption had nothing to do with the effects. Mass spectroscopy showed that the oxygen impurity of the nitrogen gas flow we used did not exceed 0.05% . A simple calculation shows that in that case absorption may account for mass increase of the sample but within the range of the measurement error $\Delta y = 0.01$. Taking into con-

sideration the results of [5], we see that the thermal effect of absorption may not exceed $\Delta H \approx 1.5$ J/g, which is by an order of magnitude less than what we have experimentally obtained.

After the exothermal peaks, further heating as a rule brings about broad endotherms on the DSC curves. This corresponds to an oxygen escape from the samples and the sample mass decreases. To avoid having to consider this process, we stopped heating right after the exothermal processes were over.

X-ray measurements are very important for understanding the observed phenomena, as well as the data we obtained on heat-release kinetics and the ΔH vs. y function.

One can *a priori* assume that the energy of the samples saved during the quenching which is later released in the form of heat, is determined by the non-equilibrium nature of lattice and/or the location of the most mobile elements, atoms of oxygen (oxygen subsystems).

In a quenched solid the energy is being saved due to the elastic distortion of the lattice and various defects of packing whose non-equilibrium distribution (corresponding to T_q) is fixed by quenching. The heating leads to relaxation of the structure, removal of distortions and redistribution of defects.

The X-ray measurements on a series of $Ba_2YCu_3O_y$ samples similar to those investigated in the present work, both quenched and heated in DSC mode (see Fig. 2, solid and dashed lines, respectively) were carried out. The data obtained, such as constancy of lattice parameters, etc., show that no significant structure relaxation takes place in the quenched samples while heating*. Similar conclusions could be drawn from the results of neutron diffraction measurements [11].

DSC is a simple technique of measuring the activation energy of heat release [14]. For this purpose, we heated the series of samples of the same composition $Ba_2YCu_3O_{6.73}$ at different heating rates in the range $\nu = 5 \dots 40$ deg/min. The shift of T_{max} thus obtained (see Fig. 2) allowed us to plot the measured dependence $\ln \nu (1/T_{max})$. As Fig. 3 shows, the latter proved to be linear which is typical for an Arrhenius process with independent motion of kinetic units.

A simple expression relates the activation energy of the exothermal process to the slope of this dependence:

$$Q = -R \frac{d \ln \nu}{d(1/T_{max})}$$
 We obtained $Q \cong 1.5$ eV. This value corresponds to the activation energy of atomic oxygen diffusion in this lattice, which lies according to different estimates in the range of $1.3 \div 1.7$ eV [15, 16]. Therefore the discovered

* The authors are grateful to S. K. Phylatov and T. V. Grachev for the possibility to get acquainted with the results obtained in X-ray diffraction measurements.

effect is related to the diffusive redistribution of atoms in the non-equilibrium oxygen subsystem.

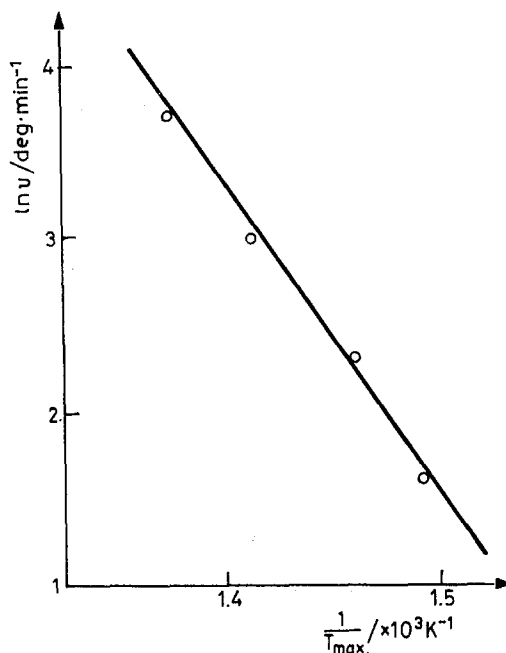


Fig. 3 Exothermal peak maximum as a function of heating rate for the quenched $Ba_2YCu_3O_y$ samples

Figure 4 shows the dependence of the heat release ΔH on the measured oxygen content for quenched samples of $Ba_2YCu_3O_y$. This dependence is of extremal nature. ΔH reaches a maximum at $y=6.4 \div 6.5$ and vanishes both at $y=6.8 \div 6.93$ and $y=6.2$.

The analysis of the data in terms of the nature of filling in oxygen positions [10] allows us to suggest the following mechanism of reorganization in the oxygen subsystem in the quenched samples of $Ba_2YCu_3O_y$.

The quenching fixes the distribution of oxygen atoms in 0, 1/2, 0 ('chains') and 1/2, 0, 0 ('channels') positions typical for high temperatures with approximately equal concentrations of atoms in each position at T_q . At lower temperatures there is no equilibrium with an excess of oxygen in the 'channels'.

When quenched samples are being heated, at the 'unfreezing' temperature of the atomic diffusive mobility of oxygen, the surplus oxygen atoms start to hop from 'channels' to 'chains', i.e. reorganization of the oxygen subsystem takes place. Since the binding energy of oxygen in the lattice is higher in 'chains' than

in 'channels', this process leads to a more stable energetic state and therefore is accompanied by an energy release.

In view of this, the extremal shapes of the $\Delta H(y)$ curve may be accounted for as follows.

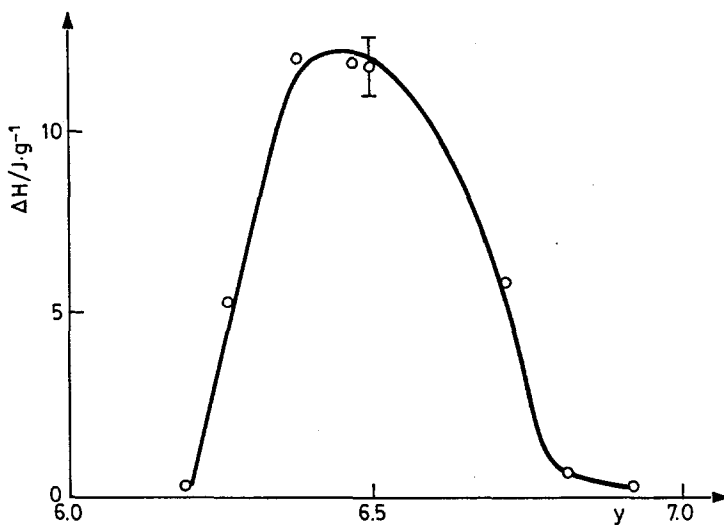


Fig. 4 Dependence of the heat release (exothermal peak area on DSC curves) on the oxygen content y for quenched $Ba_2YCu_3O_y$ samples

At high concentrations of oxygen ($y=6.8\div 6.93$) the oxygen population is rather extensive and therefore the quenching would hardly lead to any significant disbalance in oxygen distribution. As a result, DSC curves of the quenched samples bear practically no trace of exothermal effect. At low concentrations of oxygen ($y=6.2$) the heat release is also small but the reason is apparently different: the diffusing oxygen atoms are too few.

The maximum in exothermal effect at an intermediate oxygen concentration may be explained by the optimal relation between these competing factors which influence the process of oxygen subsystem reorganization: besides a considerable number of kinetic units (oxygen atoms), the degree of disbalance of the subsystem in the quenched samples is also rather high. Therefore the degree of heat-induced reorganization of the oxygen subsystem is the highest at $y=6.5$.

Energetic characteristics of hydrogenated samples

In Fig. 5 are presented the DSC curves of hydrogenated $Ba_2YCu_3O_y$ samples with varying oxygen content. The heat release at a constant value of y evidently

takes place like in the case of the quenched samples. With the hydrogenated samples, however, there are three specific features:

1. ΔH is nearly an order of magnitude higher than in the case of the quenched samples;
2. There are definitely two stages of heat release (peaks at $T_{\max,1}$ and $T_{\max,2}$);
3. The range of heat release lies at somewhat lower temperatures. For instance, $T_{\max,1} \approx 550$ K, and the left wing of this peak may vanish at approximately 450 K; these ranges are about 200 K lower than the respective values for the exotherm for the quenched samples (compare Figs 2 and 5).

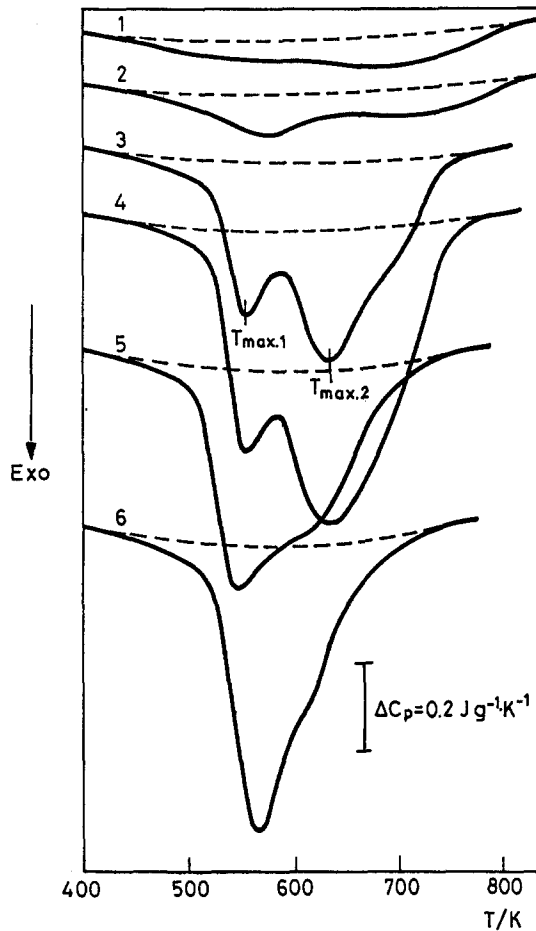


Fig. 5 DSC curves for hydrogenated $\text{Ba}_2\text{YCu}_3\text{O}_y$ samples with different oxygen content: $y = 6.77$ (1); 6.73 (2); 6.66 (3); 6.46 (4); 6.10 (5), and 5.90 (6). Heating rate: 40 deg/min. Dashed lines correspond to scan II

It is seen in Fig. 5 that the intensity of the peak corresponding to the first stage of heat release shows a monotonous growth with decrease of oxygen content. At the same time, the intensity of the peak corresponding to the second stage varies similarly to that of a single-stage Arrhenius heat release from the quenched samples. In other words, the intensity of the second peak reaches a maximum at $y = 6.5$.

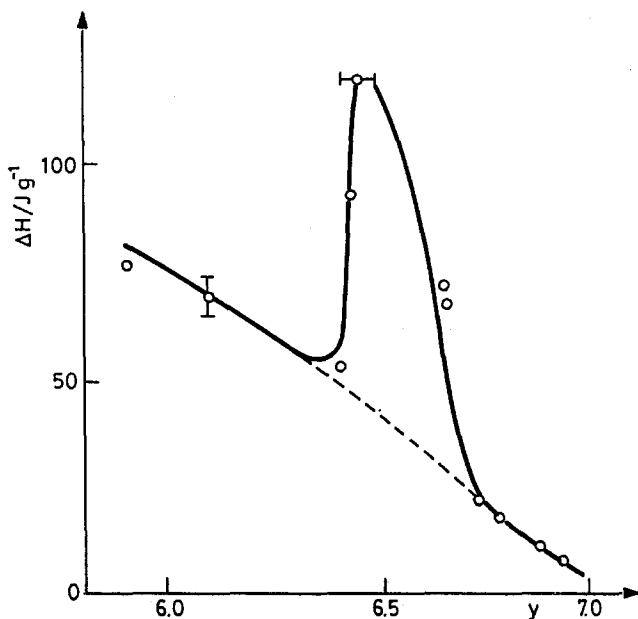


Fig. 6 Dependence of the heat release on the oxygen content y for hydrogenated $\text{Ba}_2\text{YCu}_3\text{O}_y$ samples

The dependence of ΔH on y is also characteristic. Figure 6 shows that as the oxygen content in the hydrogenated samples decreases, a monotonous increase of ΔH at the expense of the first stage of the heat release process and the pronounced peak of ΔH on this background at $y = 6.4-6.7$ at the expense of the heat release in the second stage are observed. Maximum value of $\Delta H = 115 \text{ J/g}$ is reached at $y = 6.45$.

We have found that the heating of $\text{Ba}_2\text{YCu}_3\text{O}_y$ samples hydrogenated in different ways is accompanied either by two-stage or one-stage (as for quenched samples) exothermal effect, the last being characteristic of the samples hydrogenated at the higher temperatures.

Figure 7 shows the possibility of the separate observation of the heat release stages in the samples of $\text{Ba}_2\text{YCu}_3\text{O}_y$ under study. Heating only up to 580 K is seen

to allow to fix the effect corresponding to the first stage of the process, as well as repeated heating only the second stage (curves 1, 2).

It should be noted that the latter is reached in a different way, – namely by the short-term immersion of the hydrogenated samples in liquid helium (curve 3). This interesting fact should be studied in more detail. We would like only to note that the cooling of $\text{Ba}_2\text{YCu}_3\text{O}_y$ to low temperatures may result in changes of the properties of these materials, which have been found by means of DSC and other techniques and also in connection with the oxygen subsystem instability [17, 18].

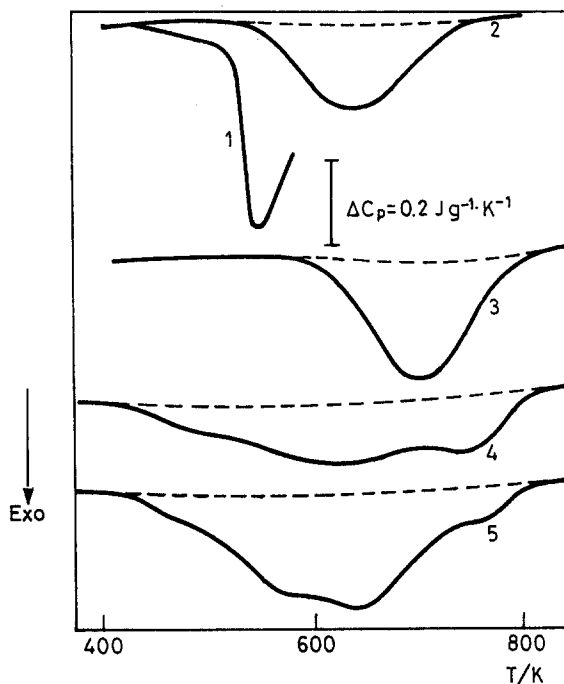


Fig. 7 DSC curves for $\text{Ba}_2\text{YCu}_3\text{O}_y$ samples treated in dihydrogen (1–3) and carbon monoxide (CO) (4,5). Heating rate: 20 deg/min. Dashed lines correspond to scan II. 1 – $y=6.45$, heating only up to 580 K; 2 – the same sample, scan II; 3 – the same as 1 with five minute immersion in liquid helium; 4 – $y=6.56$; 5 – $y=6.26$

Curves 4 and 5 in Fig. 7 show further complication of the heat release process for the samples in which the chemical extraction of oxygen was performed by another reducing agent – carbon monoxide (CO). In this case the exothermic curve contains four overlapping peaks.

The data processing technique applicable to chemical reaction analysis [19] was used for determining the kinetic parameters of the two-stage exothermal pro-

cess. The DSC curve obtained at a heating rate of 5 deg/min, when the overlap of the exothermal peaks is small,* was used.

The kinetic equation of the reaction may be written as

$$\frac{d\alpha}{dt} = K(T) \cdot (1 - \alpha)^n, \quad (1)$$

where α is the extent of the conversion, n is the reaction order, $K(T)$ is a rate constant and according to the Arrhenius equation

$$K(T) = Z \exp(-Q/RT) \quad (2)$$

where Z is the preexponential factor and Q is the activation energy of the process.

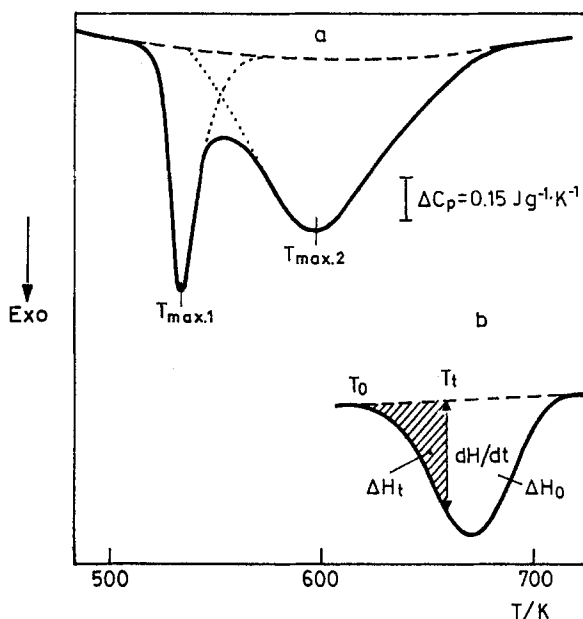


Fig. 8 DSC curves for hydrogenated $\text{Ba}_2\text{YCu}_3\text{O}_{6.66}$ sample obtained with a heating rate of 5 deg/min (a), and schematic DSC curve illustrating the calculation of kinetic parameters of the heat release process (b)

In DSC technique α is substituted by the relation $\Delta H_t / \Delta H_0$, where ΔH_t is the process heat released during the time t in the temperature range $T_0 - T_t$ (it corre-

* Further decrease of the heating rate is prevented by the base line drift during prolonged scanning in a wide temperature range.

sponds to the dotted area of the peak in Fig. 8b) and ΔH_0 is the total exothermal effect of the process (total area of the peak). The conversion rate $d\alpha/dt$ in Eq. (1) is equal to the heat flow dH/dt , normalized on the total heat of process ΔH_0 , i.e.

$$\frac{1}{\Delta H_0} \frac{dH}{dt} = K(T) \cdot (1 - \Delta H/\Delta H_0)^n. \quad (3)$$

This relation allows to calculate the dependence of K on T from the experimental DSC curve using the values obtained for dH/dt , ΔH_t , and ΔH_0 .

By adjusting n , corresponding to the linear character of this dependence in the Arrhenius coordinates $\ln K(1/T)$, the activation energy Q is determined from the relation $Q = -\frac{R d \ln K}{d(1/T)}$. The intercept of the $\ln K(1/T)$ line is equal to Z .

The technique described for the calculation of the kinetic parameters is suitable for the description of a multi-stage process and relation (2) is valid for each stage. It is only necessary to perform the procedure of peak separation with adjusting the parameter n , while the linear dependence $\ln K(1/T)$ is kept in the entire temperature range.

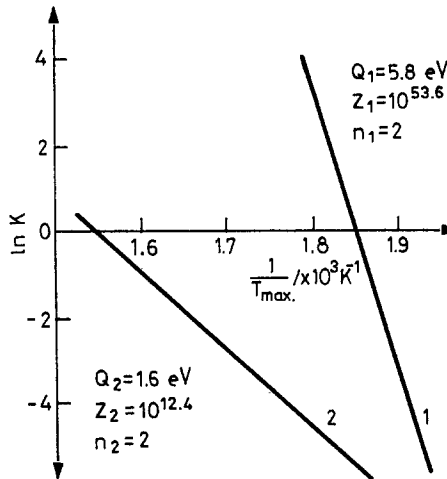


Fig. 9 Temperature dependences of the rate constants for the first (1) and second (2) stages of the process shown in Fig. 8a

Figure 9 shows these dependences for $\ln K_1$ and $\ln K_2$ obtained as a result of separation of the two-stage exothermal curve in the way shown in Fig. 8a; n appeared to be approximately equal to 2 and the $K_1(T)$ dependence corresponds to the rate constant of the first stage (peak with T_{max_1}), and the $K_2(T)$ dependence is related to the second stage (peak with T_{max_2}). The values of kinetic parameters, calculated from the linear dependences $\ln K(1/T)$ are shown in Fig. 9.

Let us next analyze the results obtained for hydrogenated samples. The activation energy for the second stage of heat release corresponds to the activation energy of the process of non-equilibrium oxygen subsystem reorganization in quenched samples $\text{Ba}_2\text{YCu}_3\text{O}_y$, i.e. the effect is also defined by the transition of excessive oxygen atoms from 'channels' to 'chains'. The values $Q_2 = 1.6$ eV and $Z_2 = 10^{12.4}$ evidence the quasi-independent, noncorrelated character of the motion of oxygen atoms during diffusion in the lattice in this case.

In the meantime, a different picture is observed for the first stage of exothermal process characteristic only of hydrogenated samples: unusually high values of the preexponential $Z_1 = 10^{53.6}$ and effective activation energy $Q_1 = 5.8$ eV evidence the co-operative character of this process.

From an analysis of the activation energy spectra for such cooperative processes, for example, carried out with DSC [19, 20], it follows that the effective activation energy determines in this case the potential barrier, being the sum of the motion barriers of several kinetic units, simultaneously or correlatively participating in the act of motion. The interdependent shift of several oxygen atoms from a certain quasi-stable state to another one seems to take place in this case. A fairly narrow peak with T_{\max_1} (Fig. 8a) is also characteristic of cooperative processes [19].

The presence of the co-operative exothermal process in hydrogenated samples, being 'trigger' for the manifestation of a higher temperature exothermal effect, could be explained in following way.

Metastable state appears as a result of low-temperature ($T \leq 500$ K) chemical extraction of part of the oxygen by hydrogen ('chemical quenching') out of $\text{Ba}_3\text{YCu}_3\text{O}_y$. Unlike the removal of oxygen by thermal treatment in inert atmosphere with following quenching, in this case 'freezing' is observed both for the atomic subsystem and the part of electronic subsystem responsible for superconductive properties. It manifests itself in two phenomena: the superconductivity is kept at the original level or close to it ($T_c = 70\text{--}90$ K) as well as the important lattice parameter C , corresponding to the interlayer distance does not change; however, the value of y decreases from 6.9 to 6.3 due to hydrogen treatment [3, 4, 13]. Sample heating over 670 K is accompanied besides the exothermal effect by the transition into the more stable state, characteristic of the samples after thermovacuum treatment: T_c decreases abruptly and C increases.

High ΔH values for hydrogenated samples show that the energy accumulated by 'chemical quenching' is much more than in the case of thermally quenched samples.

The energy release in the co-operative process with T_{\max_1} may be probably connected with the behaviour of bridge oxygen atoms O(A) in the line Cu(1) – O(A) – Cu(2) according to the model of two-well potential for this oxygen proposed by us [7–9]: two potential minima are determined here by the oxygen co-ordination of copper in the chain. Oxygen O(A) is usually considered to be of

the most significance in the process of charge transport between the chains Cu(1) – O and planes Cu(2) – O...[21].

There are considerations to suppose the shape and depth of potential well for O(A) change essentially at varying oxygen content and degree of order in chains Cu(1) – O.

Overcoming of the barrier between two potential minima in the model [7–9] with transition of the atoms O(A) to lower energetic state obviously determines the first exothermal peak on DSC curves for hydrogenated samples. If the vacancy groups in the chains appear in Ba₃YCu₃O_y as a result of inhomogeneous oxygen extraction by hydrogen, the co-operative oxygen transport effects seem to be possible.

References

- 1 J. G. Bednorz, and K. A. Müller, *Z. Phys. B. Cond. Mat.*, 64 (1986) 189.
- 2 O. K. Antson, P. E. Hiismaki, H. O. Poyry *et al.*, *Solid State Commun.*, 64 (1987) 757.
- 3 Yu. M. Baykov, S. L. Shohor, F. A. Chudnovskii *et al.*, *Superconductivity: Phys. Chem. Techn.*, (in Russian) 3 (1990) 2090.
- 4 Yu. M. Baykov, S. K. Phylatov, V. V. Semin *et al.*, *Pisma Zh. Techn. Fiz.*, 16 (1990) 76.
- 5 H. V. Krebs and O. Bremert, *J. Less-Common Metals*, 150 (1989) 159.
- 6 B. A. Glawacki, R. I. Highmere, K. F. Peters *et al.*, *Supercond. Sci. Technol.*, 1 (1988) 7.
- 7 Yu. M. Baykov, F. A. Chudnovskii, V. A. Bershtein *et al.*, In: *Abstr. of Sov.-Germ. Seminar of HTSC*, Karlsruhe, BRD October 1990.
- 8 Yu. M. Baykov, F. A. Chudnovskii, V. A. Bershtein *et al.*, In: *Abstr. of Appl. HTSC Conf. Colorado, USA September 1990*, p. 43.
- 9 Yu. M. Baykov, F. A. Chudnovskii, V. A. Bershtein *et al.*, In: *Abstr. Intern. Conf. "Sol. St. Chem."*, Odessa, USSR Oct. 1990, p. 148.
- 10 J. E. Gruboy, A. P. Kaul and Yu. G. Metlin, *Khimia tverdogo tela, VINITI, Moskva* 6 (1989) 25, 27, 37.
- 11 C. Greaves and P. R. Slater, *Solid State Commun.*, 74 (1990) 591.
- 12 V. F. Degtyaryeva, O. V. Zharikov, J. N. Kremenskaya *et al.*, *Solid State Commun.*, 70 (1989) 561.
- 13 Yu. M. Baykov, S. K. Phylatov, V. V. Semin *et al.*, *Pisma Zh. Tekhn. Fiz.*, 16 (1990) 56.
- 14 M. De Bolt, A. Eastel, P. Macedo and C. Moynihan, *J. Amer. Cer. Soc.*, 59 (1976) 16.
- 15 Yu. M. Baykov, B. M. Elkin, S. E. Nikitin *et al.*, *Pisma Zh. Tekhn. Fiz.*, 14 (1988) 1816.
- 16 Y. Ikuma and S. Akiyoshi, *J. Appl. Phys.* 64 (1988) 3915.
- 17 V. A. Bershtein, A. A. Guryanov, V. M. Egorov *et al.*, *Fizika tverdogo tela*, 31 n8 (1989) 221.
- 18 I. G. Gusakovskaya, S. I. Pyrumova, V. V. Tkachev *et al.*, *Inst. Chem. Phys. Chernogolovka. Prepr.* (1989) 16p.
- 19 V. A. Bershtein and V. M. Egorov, *Differential Scanning Calorimetry in the Physics and Chemistry of Polymers, Khimia, Leningrad* 1990, p. 255.
- 20 V. A. Bershtein, and V. M. Egorov, *Fizika tverdogo tela*, 26 (1984) 1987.
- 21 R. J. Cava *et al.*, *Physica C.*, 156 (1988) 523.

Zusammenfassung — Für eine Reihe von Verbindungen der allgemeinen Formel Ba₂YCu₃O_y und einem Sauerstoffgehalt von y=6.0...6.9 wurden mittels verschiedener Wärmebehandlungen bei 800-1200 K, gefolgt durch Abschrecken oder beim chemischen Sauerstoffentzug durch Einbringen der Probe in Diwasserstoff bei 470-490 K DSC-Untersuchungen

durchgeführt. Wird die Probe in Stickstoff erhitzt, so behält sie ihren Sauerstoffgehalt bei und zeigt bei 450-850 K einen exothermen Effekt. Es wurde gezeigt, daß die Funktion $\Delta H(y)$ bei etwa $y=6.5$ ein Maximum erreicht. Kinetische Messungen zeigen, daß für diesen Effekt die diffusive Beweglichkeit der Sauerstoffatome im Gitter verantwortlich ist.